

International Conference on Laser Applications at Accelerators, LA3NET 2015

Numerical study of a multi-stage dielectric laser-driven accelerator

Yelong Wei^{a,b*}, Guoxing Xia^{a,d}, Jonathan. D. A. Smith^e, Kieran Hanahoe^{a,d}, Oznur Mete^{a,d}, Steve P. Jamison^{a,c}, Carsten P. Welsch^{a,b}

^a*Cockcroft Institute, Daresbury, Warrington, WA4 4AD, UK*

^b*University of Liverpool, Liverpool, Merseyside L69 3BX, UK*

^c*Accelerator Science and Technology Centre, Daresbury, Warrington, WA4 4AD, UK*

^d*University of Manchester, Manchester, M13 9PL, UK*

^e*Tech-X UK Ltd, Sci-Tech Daresbury, Warrington, UK*

Abstract

In order to overcome the limits of commonly used radiofrequency accelerators, it is highly desirable to reduce the unit cost and increase the maximum achievable accelerating gradient. Dielectric laser-driven accelerators (DLAs) based on grating structures have received considerable attention due to maximum acceleration gradients of several GV/m and mature lithographic techniques for structure fabrication. This paper explores different spatial harmonics excited by an incident laser pulse and their interaction with the electron beam from the non-relativistic (25 keV) to the highly relativistic regime in double-grating silica structures. The achievable acceleration gradient for different spatial harmonics and the optimal compromise between maximum acceleration gradient and simplicity of structure fabrication are discussed. Finally, the suitability of a multi-stage DLA which would enable the acceleration of electrons from 25 keV to relativistic energies is discussed.

© 2015 The Authors. Published by Elsevier B.V. This is an open access article under the CC BY-NC-ND license (<http://creativecommons.org/licenses/by-nc-nd/4.0/>).

Peer-review under responsibility of the University of Liverpool

Keywords: Dielectric laser-driven accelerator (DLA); micro accelerators; electron beam; compact radiation source; multi-stage acceleration; high acceleration gradient; relativistic particle beam.

* Corresponding author. Tel.: +44 01925 864055
E-mail address: yelong.wei@cockcroft.ac.uk

1. Introduction

Dielectric laser-driven accelerators (DLA) are strong potential candidates for ultra-compact electron accelerators and might even open up new avenues for future high energy physics accelerators and free-electron lasers. Due to a much higher damage threshold ($0.2\text{-}2 \text{ J/cm}^2$) than metals, dielectric microstructures can support accelerating fields that are orders of magnitude higher than what can be achieved in conventional radio-frequency cavity-based accelerators. They can therefore support acceleration gradients up to several GV/m . Many candidates for DLAs have been proposed so far: Grating-based structures [1]-[6], photonic crystal structures [7][9] and woodpile structures [10]. A proof-of-principle experiment has successfully demonstrated acceleration of relativistic electrons with an accelerating gradient of 250 MeV/m [11] in a fused silica double-grating structure and the acceleration of non-relativistic 28 keV electrons through a single-grating structure was also observed [12]. These two experiments demonstrate the possibility of an all-optical DLA for full energy acceleration in the future.

The geometry with two gratings facing each other is called a double-grating structure, which was originally proposed by Plettner [1] as shown in Fig. 1. Initial studies into these double-grating structures have already been performed by the authors with the aim to increase the acceleration efficiency for highly relativistic and non-relativistic electrons [13]. This paper investigates a grating-based multi-stage DLA from 25 keV ($\beta = v/c = 0.3$, where v is the electron velocity and c the speed of light) to the highly relativistic regime where $\beta \approx 1$. In particular, the different spatial harmonics excited by the diffraction of an incident laser pulse are analysed. In a second step the achievable acceleration gradient, as identified through simulations for different spatial harmonics, will be discussed. On this basis, an optimal compromise between maximum acceleration gradient and simplicity of structure fabrication is proposed for a novel structure that would be suitable to accelerate electrons from 25 keV to highly relativistic energies.

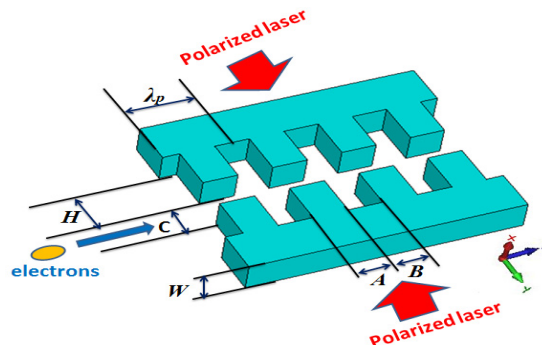


Fig. 1. Schematics of a dielectric double-grating structure excited symmetrically by laser beams. λ_p , C, H and W represent grating period, vacuum channel width, pillar height and dielectric wall width.

2. Accelerating Field Simulation

The VSIM code [14] based on the finite-difference time domain (FDTD) method has been used to precisely calculate the electric field distribution in the 2-dimensional geometry of the double-grating structure. The acceleration gradient G_0 was evaluated by $E[z(t), t]$ which is the electric field distribution along the vacuum channel center as shown in Fig. 2 (c) using

$$G_0 = \frac{1}{\lambda_p} \int_0^{\lambda_p} E[z(t), t] dz, \quad (1)$$

where λ_p is the grating period and, $z(t)$ is the position of electrons at time t . Silica-grating structures generating $G_0=0.5 E_0$ [1], where E_0 is the input laser electric field, have been reported. This value can be doubled [4],[5] by illuminating the structure from both sides. The other important factor is the acceleration efficiency, given by $\eta = G_0/E_{max}$ and is used to evaluate the maximum achievable acceleration gradient, where E_{max} is the maximum electric field generated by the laser electric field E_0 in the material.

When a double-grating structure is driven by two linearly polarized laser beams with the electric field along the z axis from opposite sides, the diffraction of the incident laser at the grating excites different spatial harmonics which can be used to accelerate the electrons, as shown in Fig. 2 (a) and (b). The grating period λ_p , laser wavelength λ_0 and electron velocity v , $\beta=v/c$ have met the synchronicity condition [2]: $\lambda_p = n \cdot \beta \cdot \lambda_0$ where n is the numbers of laser cycles per electron passing one grating period.

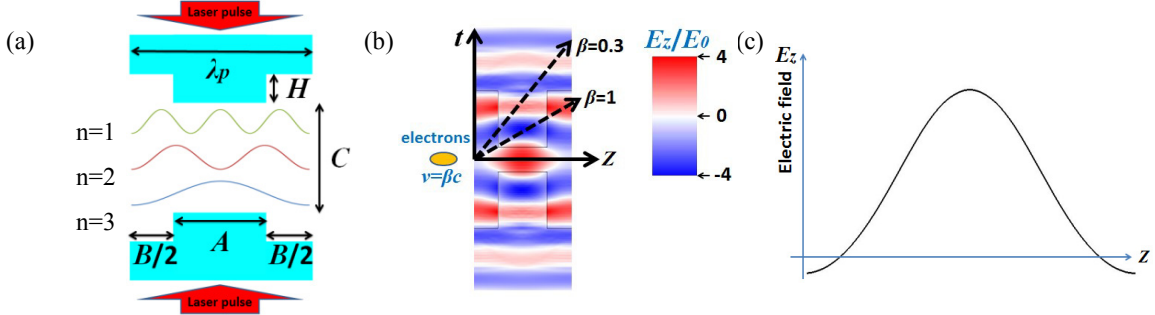


Fig. 2. (a) Illustration of the first, second and third spatial harmonics for the case that one grating period is illuminated by laser from two sides, in which they have the same frequency of c/λ_0 but different wavelength due to diffraction; (b) Dotted arrows indicate injection electrons with different speed $\beta=0.3, 1$ respectively; (c) The longitudinal electric field distribution E_z at the frequency of c/λ_0 along the vacuum channel.

3. Multi-stage DLA Analysis

A two-stage DLA consisting is proposed here: A first-stage non-relativistic DLA from 25 keV to 1 MeV as shown in Fig. 3, and a second-stage relativistic DLA from 1 MeV to relativistic energies. Optimization studies have been carried out for the acceleration of highly relativistic [1][4][5][13] and non-relativistic electrons (25 keV, $\beta=0.3$) [13] in a double-grating structure. It was found that the first spatial harmonics have the largest acceleration efficiency to interact with 25 keV electrons ($\eta=0.04$) as compared to the second spatial harmonics ($\eta=0.03$) and third spatial harmonics ($\eta=0.02$) as shown in Fig. 4 (d). In the simulation, a laser with a wavelength of $\lambda_0=1550$ nm is used to excite the grating structure from two sides. Silica (SiO_2 , refractive index $n=1.528$ [15]) was chosen as grating structure material due to its transparency, high damage threshold, low thermal conductivity, low nonlinear optical coefficients and chemical stability.

In the first acceleration stage, different spatial harmonics are excited that can be used to accelerate electrons from 25 keV to 1 MeV, provided that the synchronicity condition $\lambda_p = n \cdot \beta \cdot \lambda_0$ is fulfilled. The ratio of the pillar width to the grating period A/λ_p , as well as the pillar height H were optimized to maximize the acceleration gradient for different velocities, ranging from $\beta=0.3$ to $\beta=0.9$. First, the pillar height H was varied between 0 and λ_p using a fixed pillar ratio of $A/\lambda_p=0.5$. In a next step the pillar ratio A/λ_p was changed between 0 and 1 for the optimum pillar height. Fig. 4 (a) and (d) show the acceleration gradient and acceleration efficiency η as a function of the electron energy exploiting the first, second and third spatial harmonics in a double-grating structure with a vacuum channel width of 200 nm. It can be seen that acceleration gradient and efficiency η gradually increase with electron energy due to wave matching between the wave vector of the incident laser k_0 and the synchronous spatial harmonics $k=k_0/\beta$.

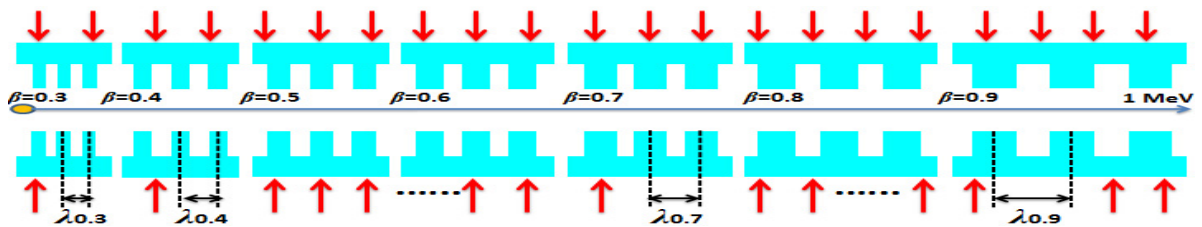


Fig. 3. Sketch of the first-stage non-relativistic DLA, where red arrows represent the laser beams from two sides.

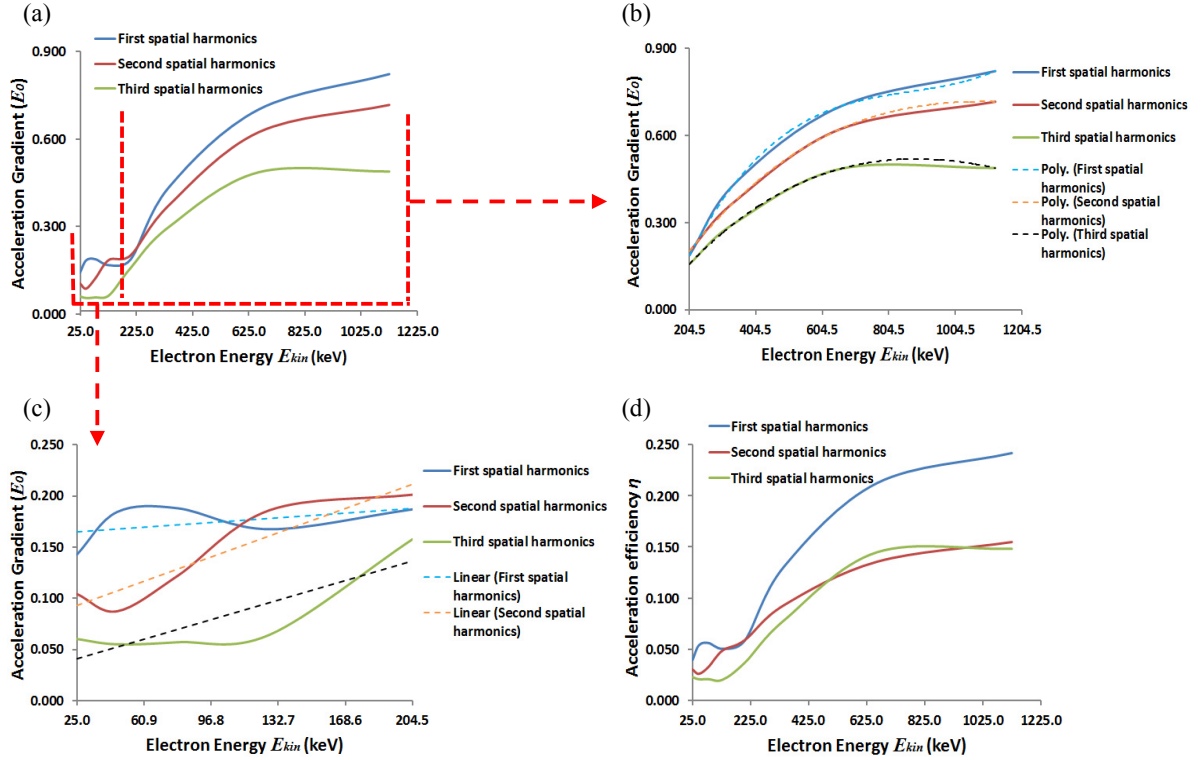


Fig. 4. Acceleration gradient (a) and efficiency η (d) as a function of electron energy for the first (c) and second part (b) of a DLA, respectively.

As shown in red rectangular regions of Fig. 4(a), a DLA that accelerates from 25 keV to 1 MeV was divided into two sections, ranging from 25 keV to 204.5 keV, i.e. $\beta=0.7$, and from 204.5 keV to 1 MeV. Fig. 4 (c) shows the different linear fits that approximate the relationship between acceleration gradient and electron energy from 25 keV to 204.5 keV: $G/E_0 = k_0 + E_{kin} \cdot k_1$, combining these equations with the definition of the acceleration gradient G

$$\frac{dE_{kin}}{dz} = e \cdot G, \quad (2)$$

yields the solution $E_{kin} = (E_{kin}^i + k_2) \cdot \exp(eE_0 \cdot z \cdot k_3 \text{ eV}^{-1}) - k_2$. Here, k_0 , k_1 , k_2 and k_3 are shown in Table 1, E_{kin}^i with units of keV is kinetic energy of the electrons at injection, E_0 with units of V/m is the input laser electric field and z represents moving direction for electrons. So the estimated lengths of this DLA structure for all three spatial harmonics are shown in 0.

Table 1. The different value k_0, k_1, k_2, k_3 for different spatial harmonics

	k_0	k_1	k_2	k_3
First spatial harmonics	0.1615	10^{-4}	$0.1615 \cdot 10^4$	10^{-7}
Second spatial harmonics	0.0766	$7 \cdot 10^{-4}$	$0.0109 \cdot 10^4$	$7 \cdot 10^{-7}$
Third spatial harmonics	0.0276	$5 \cdot 10^{-4}$	$0.0055 \cdot 10^4$	$5 \cdot 10^{-7}$

Table 2. Estimated length of a DLA for different spatial harmonics that accelerates from 25 keV to 204.5 keV.

$E_{kin}^i = 25 \text{ keV} (\beta=0.3),$ $E_{kin} = 204.5 \text{ keV} (\beta=0.7)$	$E_0 = 1 \text{ GV/m}$	$E_0 = 2 \text{ GV/m}$
First spatial harmonics	1.039 mm	0.519 mm
Second spatial harmonics	1.214 mm	0.607 mm
Third spatial harmonics	2.353 mm	1.177 mm

For the second DLA structure that accelerates from 204.5 keV to 1 MeV, as shown in Fig. 4(b), different equations can be obtained from the polynomial fit: $G/E_0 = m_0 \cdot (E_{kin})^3 - m_1 \cdot (E_{kin})^2 + m_2 \cdot E_{kin} - m_3$. Following the same approach as above, the solving equation is

$$\int_{E_{kin}^{ii}}^{E_{kin}^i} [1/(m_0 \cdot E_0 \cdot (E_{kin})^3 - m_1 \cdot E_0 \cdot (E_{kin})^2 + m_2 \cdot E_0 \cdot E_{kin} - m_3 \cdot E_0)] dE_{kin} = z,$$

where m_0, m_1, m_2, m_3, m_4 are shown in Table 3, E_{kin}^{ii} with units of keV represents the kinetic energy of the electrons upon injection into the second DLA structure, E_0 with units of V/m is the input laser electric field and z represents moving direction for electrons. Based on these equations, the estimated length of a non-relativistic DLA from 204.5 keV to 1 MeV was calculated and is shown in 0.

Table 3. The different value m_0, m_1, m_2, m_3 for different spatial harmonics

	m_0	m_1	m_2	m_3
First spatial harmonics	$2 \cdot 10^{-9}$	$4 \cdot 10^{-6}$	0.0037	0.4051
Second spatial harmonics	$3 \cdot 10^{-10}$	10^{-6}	0.002	0.1435
Third spatial harmonics	$3 \cdot 10^{-10}$	10^{-6}	0.0017	0.134

Table 4. Estimated length of a DLA for different spatial harmonics that accelerates from 204.5 keV to 1 MeV

$E_{kin}^{ii} = 204.5 \text{ keV} (\beta=0.7)$ $E_{kin} = 1 \text{ MeV}$	$E_0 = 1 \text{ GV/m}$	$E_0 = 2 \text{ GV/m}$
First spatial harmonics	1.223 mm	0.611 mm
Second spatial harmonics	1.284 mm	0.642 mm
Third spatial harmonics	1.656 mm	0.828 mm

It can be seen from 0 and 0 that the first spatial harmonics was more efficient to accelerate electrons from 25 keV to 1 MeV as compared to the second and third spatial harmonics. The corresponding DLA lengths are 2.262 mm, 2.498 mm and 4.009 mm, respectively, when the input laser electric field E_0 is 1 GV/m. However, the fabrication of a grating with a period of $465=1 \cdot 0.3 \cdot 1550 \text{ nm}$ is a significant challenge when we choose the first spatial harmonic to accelerate 25 keV electrons. In order to reduce the fabrication effort considerably, the second spatial harmonics with an initial grating period of $930=2 \cdot 0.3 \cdot 1550 \text{ nm}$ is a good compromise. Combining both results yields a combined non-relativistic DLA as shown in Table 5. This accelerator is composed of two parts covering the before-mentioned energy regimes.

Table 5. Estimated total length of a DLA that accelerates electrons from 25 keV to 1 MeV.

	$E_0 = 1 \text{ GV/m}$	$E_0 = 2 \text{ GV/m}$
From 25 keV to 204.5 keV using the second spatial harmonics	1.214 mm	0.607 mm
From 204.5 keV to 1 MeV using the first spatial harmonics	1.223 mm	0.611 mm
Total DLA length	2.437 mm	1.218 mm

In the second-stage electrons are accelerated from 1 MeV to highly relativistic energies. The acceleration gradient G roughly equals E_0 [4][5] when illuminated from two sides and hence the length of the relativistic DLA can be obtained. As shown in Table 6, the estimated length scales linearly with the final energy of the relativistic electrons and inversely with the laser input electric field.

Table 6. Estimated length of a relativistic DLA for different final energies of the electron beam.

Final electron energy E_{kin}^f	$E_0 = 1 \text{ GV/m}$	$E_0 = 2 \text{ GV/m}$
100 MeV	0.10 m	0.05 m
1 GeV	1.00 m	0.50 m
10 GeV	10.0 m	5.00 m

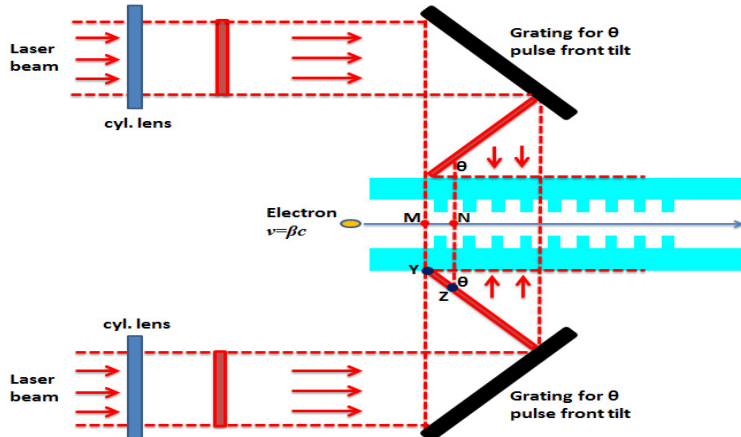


Fig. 5. The setup of multi-stage DLA with front tilt grating, where red arrows represent laser beams.

In practice for a multi-stage DLA, a mechanism [1] to efficiently overlap the accelerating electric field with the electron beam along the vacuum channel is required and the laser pulse front needs to be adjusted. This can be realized by means of rotatable gratings as depicted in Fig. 5.

For a sufficiently short electron bunch with $v = \beta \cdot c$ that is travelling from point M to N in one grating period, the velocity of the electrons can be assumed to be almost constant, $\Delta\beta/\beta \sim 0$. This is true for relativistic electrons where $\beta \sim 1$, as the change in velocity is practically zero. But also in the non-relativistic case the energy gain over one grating period λ_g is well below several keV, so that the velocity of electrons can be assumed constant. As shown in Fig. 5, there is some time delay for the pulse front at points Y and Z to arrive at points M and N, respectively. The time delay between Y and Z is:

$$c \cdot \Delta t = \lambda_g \cdot \tan\theta \quad (3)$$

At Δt the electrons have travelled from M to N:

$$\lambda_g = v \cdot \Delta t. \quad (4)$$

Thus

$$\beta = v/c = 1/\tan\theta. \quad (5)$$

This shows that the angle of the pulse-front tilt can be adjusted to make sure that the accelerating field remains synchronized with the electron bunches. However, dephasing might become an issue for continuous acceleration in a multi-stage DLA and this will be subject to further research.

4. Laser system

In a DLA system the input laser should first be focused e.g. by a lens and then a short laser pulse can be divided into many segments and introduced into the structure to keep the maximum electric field E_{max} in the grating structure below the damage threshold E_{th} [1]. The laser pulse energy and pulse width will significantly affect the input electric field E_0 pumped into the grating structure. As shown in previous sections, a non-relativistic DLA from 25 keV to 1 MeV requires a total structure length of 2.437 mm. The corresponding laser system is shown in Table 7 and would generate an input field $E_0=1$ GV/m for a structure of 2.437 mm length and a height of 0.60 mm. The damage threshold for silica is about 1 J/cm² for laser pulses of 100 fs [16], which is equivalent to an electric field of $E_{th}=8.7$ GV/m. In this configuration even an E_0 as high as 2.0 GV/m would still not damage the silica structure.

Table 7. Overview of laser system parameters.

Laser Characteristics	
Wavelength	1550 nm
Pulse energy	~2 mJ
Pulse width	1 ps

5. Conclusion

Optimization studies for a multi-stage DLA with the aim to maximize its acceleration gradient in the energy range between 25 keV ($\beta=0.3$) and relativistic energies were presented in this paper. The proposed multi-stage DLA consists of two stages: A first, non-relativistic regime from 25 keV to 1 MeV and a second, DLA from 1 MeV to highly relativistic energies. Results from simulation studies into the different spatial harmonics were present and it was shown that the first harmonics is more efficient to accelerate electrons from 25 keV to 1 MeV as compared to the second and third spatial harmonics. However, considering fabrication limitations it was found that choosing the second spatial harmonics was the more appropriate choice.

Finally, a practical setup where the laser pulse can be changed by movable gratings was proposed. In such a scheme the synchronicity between the electron pulse and the accelerating longitudinal electric field is guaranteed by appropriate modification of the incoming laser field. However, dephasing remains a big issue for multi-stage DLA and shall be investigated in detail in the near future.

Acknowledgements

This work is supported by the EU under Grant Agreement No. 289191 and the STFC Cockcroft Institute core Grant No. ST/G008248/1.

References

- [1] Plettner T, Lu P. P, and Byer R. L. Proposed few-optical cycle laser-driven particle accelerator structure. *Phys. Rev. ST Accel. Beams* 2006; 9: 111301.
- [2] Plettner T, Byer R. L, McGuinness C, and Hommelhoff P. Photonic-based laser driven electron beam deflection and focusing structures. *Phys. Rev. ST Accel. Beams* 2009;12: 101302.
- [3] Plettner T, Byer R. L, and Montazeri B. Electromagnetic forces in the vacuum region of laser-driven layered grating structures. *J. Mod. Opt.* 2011;58: 1518.
- [4] Aimidula A, Bake M. A, Wan F, Xie B. S, Welsch C. P, Xia G, Mete O, Uesaka M, Matsumura Y, Yoshida M, and Koyama K. Numerically optimized structures for dielectric asymmetric dual-grating laser accelerators. *Physics of Plasmas* 2014;21: 023110.
- [5] Aimidula A, Welsch C. P, Xia G, Koyama K, Uesaka M, Yoshida M, Mete O, Matsumura Y. Numerical investigations into a fiber laser based dielectric reverse dual-grating accelerator. *Nucl. Instr. Meth. A* 2014; 740: 108–113.
- [6] Chang C. M and Solgaard O. Silicon buried gratings for dielectric laser electron accelerators. *Appl. Phys. Lett.* 2014;104: 184102.
- [7] Lin X. E. Photonic band gap fiber accelerator. *Phys. Rev. ST Accel. Beams* 2001;4: 051301.
- [8] Reboud V, Romero-Vivas J, Lovera P, Kehagias N, Kehoe T, Redmond G, and Torres C. M. S. Lasing in nanoimprinted two-dimensional photonic crystal band-edge lasers. *Appl. Phys. Lett.* 2013;102: 073101.
- [9] Cowan B. M. Two-dimensional photonic crystal accelerator structures. *Phys. Rev. ST Accel. Beams* 2003;6: 101301.
- [10] Wu Z, England R.J, Ng C.K, Cowan B, McGuinness C, Lee C, Qi M, and Tantawi S. Coupling power into accelerating mode of a three-dimensional silicon woodpile photonic band-gap waveguide. *Phys. Rev. ST Accel. Beams* 2014;17: 081301.
- [11] Peralta E. A, Soong K, England R. J, Colby E. R, Wu Z, Montazeri B, McGuinness C, McNeur J, Leedle K. J, Walz D, Sozer E. B, Cowan B, Schwartz B, Travish G & Byer R. L. Demonstration of electron acceleration in a laser-driven dielectric microstructure. *Nature* 2013;503: 91.
- [12] Breuer J and Hommelhoff P. Laser-Based Acceleration of Nonrelativistic Eletrons at a Dielectric Structure. *Phys. Rev. Lett.* 2013;111: 134803.
- [13] Wei Y, Welsch C.P, Xia G.X, Mete O, Hanahoe K, Smith J.D.A. Investigations into Dielectric Laser-driven Accelerators using the CST and VSIM Simulation Codes. IPAC2015 Proceedings, Richmond, VA, USA, WEPWA051
- [14] VSIM, available from www.txcorp.com.
- [15] Ghosh G. Dispersion-equation coefficients for the refractive index and birefringence of calcite and quartz crystals. *Opt. Commun.* 1999;163: 95.
- [16] Lenzner M, Krüger J, Sartania S, Cheng Z, Spielmann Ch, Mourou G, Kautek W, Krausz F. Femtosecond optical breakdown in dielectrics. *Phys. Rev. Lett.* 1998;80: 18.